frontiers | Frontiers in Energy Research

ORIGINAL RESEARCH
published: 26 May 2022
doi: 10.3389/fenrg.2022.898620

Distributionally Robust Optimal Bidding of Energy Hubs in the Joint Electricity and Carbon Market

Lifei Ma[1], *Shengwei Liu*[2]* *and Jizhen Liu*[1,2]

[1]*School of Control and Computer Engineering, North China Electric Power University, Beijing, China,* [2]*Energy and Electricity Research Center, Jinan University, Guangzhou, China*

To realize the lower carbon and more efficient operation of energy hubs in the joint electricity and carbon market, a day-ahead bidding strategy is proposed for the energy hub operator (EHO). Considering the uncertainties of prices, demands, and renewable energy sources, this strategy is formulated as a novel two-stage distributionally robust joint chance-constrained optimization problem. A total distance-based ambiguity set is proposed to preserve the mean value of uncertain factors. By introducing this indicator function, this problem is further reformulated as a mixed-integer linear programming (MILP) problem. Simulations are performed based on the electricity and carbon prices in Europe, and the relation between the carbon emission and operational cost is further investigated in the case studies.

Keywords: energy hubs, carbon, optimal bidding, uncertainties, distributionally robust

OPEN ACCESS

Edited by:
Rui Wang,
Northeastern University, China

Reviewed by:
Xuewei Pan,
Harbin Institute of Technology, China
Yalong Li,
China University of Mining and Technology, China

****Correspondence:***
Shengwei Liu
15622767651@163.com

Specialty section:
This article was submitted to Smart Grids,
a section of the journal Frontiers in Energy Research

Received: *18 March 2022*
Accepted: *11 April 2022*
Published: *26 May 2022*

Citation:
Ma L, Liu S and Liu J (2022) Distributionally Robust Optimal Bidding of Energy Hubs in the Joint Electricity and Carbon Market. Front. Energy Res. 10:898620. doi: 10.3389/fenrg.2022.898620

1 INTRODUCTION

1.1 Motivation

Energy hubs (EHs) are recognized as a powerful platform to realize the efficient energy conversion and utilization for the future low carbon society, e.g., buildings and industry parks (Mohammadi et al., 2017). With the deregulation of the energy market and the emergence of the carbon market, the energy hub operator (EHO) can participate in both electricity and carbon markets (Ding et al., 2020). It brings significant flexibility to the EHO in reducing the carbon emission (Olsen et al., 2018), while introducing additional risks to the operational cost, e.g., uncertain carbon prices (Sun and Huang, 2020). These uncertainties should be properly modeled and incorporated into the risk management scheme of EHOs.

1.2 Literature Review

The bidding strategies of EHOs within the electricity market, including the day-ahead and real-time electricity market, can always be modeled as deterministic optimization problems to reduce the operational cost (Brahman et al., 2015), emissions (Brahman et al., 2015), and maximize the utility (Li et al., 2018). A time-series technique for predicting the power generation of the photovoltaic (PV) cell is applied in (Brahman et al., 2015), and it is assumed that there is no bias from the actual renewable output to the forecast value. A mathematical program with equilibrium constraints is proposed for studying the strategic behaviors of profit-driven EHs in both the electricity and thermal markets from a deregulated market point of view, and the uncertainties of electricity and heating demand are neglected in the bidding optimization process, considering the conciseness of the model. However, one significant feature of EHs is to cope with the fluctuation and intermittency of the distributed renewable generation with the flexibility provided by multicarrier energy systems (Jadidbonab et al., 2020).

Furthermore, according to the uncertainties of renewable energy sources, loads, prices, etc., the deterministic strategies can be further extended to stochastic optimization (Davatgaran et al., 2018; Zhao et al., 2020; Jadidbonab et al., 2020), robust optimization (Lu et al., 2020), distributionally robust optimization (Zhao et al., 2019), and hybridization (Liu et al., 2021). The hybrid alternating current/direct current (AC/DC) microgrid is embedded as an electrical hub for EHs to realize the high efficiency of energy conversion, and a two-stage stochastic programming problem is proposed, where uncertain day-ahead prices, loads, PV, and ambient temperatures are depicted by scenario trees. Making full use of the thermal demand flexibility, the quality of thermal service is modeled as a chance constraint (Zhao et al., 2020). In Oskouei et al. (2021), a large set of industrial EHs are integrated into virtual EHs to trade energy in various markets, and the robust approach is coordinated with a stochastic programming model to formulate a hybrid expression of uncertainties, considering the priority of day-ahead electricity prices. The ability of EHs to participate in the joint electricity and thermal markets in the form of virtual power plants (VPPs) is explored in Jadidbonab et al. (2020), and a self-scheduling program is proposed for virtual EHs to maximize the revenue.

When the carbon emission is considered, the bidding management should consider the carbon emissions as objective functions (Yang et al., 2019) or constraints (Cheng et al., 2018). For the given carbon permit prices, a price-taker bidding strategy is proposed for the VPP operator to bid in the energy, ancillary services, and carbon market in (Yang et al., 2019), where carbon emissions, greenhouse gases, and pollutants are effectively reduced by the carbon trading mechanism. In Cheng et al. (2018), an analytical model called carbon emission flow is proposed to quantify the allocation of carbon emission among different energy carriers in delivery and conversion processes including both primary and secondary energy. This work is further used to realize the coordination between transmission and distribution systems with locational marginal electricity and uniform carbon prices in Cheng et al. (2020). Though there have been few studies about carbon trading in the existing literature, the uncertainties of carbon prices have not been considered in existing works (Yang et al., 2019; Cheng et al., 2018, 2020). It introduces additional risks to EHOs involving carbon markets.

The prevalent works on the risk hedging strategies of EHOs in various markets are to manage specific uncertainties. These uncertainties are the aggregation of prices, renewable energy output, loads, etc. They can be further depicted by the stochastic model (Zhao et al., 2020), uncertain sets (Lu et al., 2020), and ambiguity sets (Zhao et al., 2019). The required scenarios for stochastic optimization rapidly increase with a growing number of uncertainties to sustain an acceptable confidence level, or uncertainties are assumed to obey exact probability distributions which are normally unrealistic. In robust optimization, uncertainties are always depicted as an uncertainty set, e.g., polyhedron, which ignores the distribution information, and the optimized result by considering the worst condition can be overconservative. To address these limitations, the ambiguity sets are proposed under different metrics, e.g., total distance (Liu et al., 2021) and moment-based distances (Zhao et al., 2019). However, when the carbon price uncertainties are considered, the ambiguity sets have not been modeled.

To address the uncertainties under joint electricity and carbon markets, the EHO should optimize the conversion, storage, and consumption processes within EHs. As the distributed energy resources are to be integrated into EHs, the conversion process, from renewable energy sources and gas to electricity and thermal energy, has been embedded into the bidding strategies of EHOs (Davatgaran et al., 2018; Dai et al., 2017). Using existing electrical and thermal energy storage systems (ESSs), the electricity and thermal energy can be charged and discharged efficiently. The demand response programs have been considered from the energy consumption perspective, and the quality of thermal services has been utilized to reduce the operational risk (Zhao et al., 2020). The flexibility of the thermal demand has not been explored to reduce the risks under joint electricity and carbon markets.

1.3 Contributions

To manage the uncertainties in joint electricity and carbon markets, a novel day-ahead bidding strategy is proposed for the EHO. This strategy is formulated as a two-stage distributionally robust chance-constrained programming problem, where the uncertainties of prices, loads, renewable energy sources, and ambient temperature are formulated as a novel ambiguity set. The quality of service for the thermal demand is relaxed and treated as a joint chance constraint. Based on duality, the problem is reformulated as a mixed-integer linear programming (MILP) problem. The main contribution of this article can be summarized as follows:

- A novel ambiguity set is proposed for electrical prices and carbon prices. The first-order information is preserved in this set.
- A novel two-stage distributionally robust joint chance-constrained programming problem is proposed to manage the uncertainties in the joint electricity and carbon markets.

The rest of this article is organized as follows. The day-ahead bidding scheme is proposed in **Section 2**. The two-stage distributionally robust joint chance-constrained programming problem is formulated in **Section 3**. The deterministic reformulation method is given in **Section 4**. Case studies are performed in **Section 5**. Conclusions are drawn in **Section 6**.

2 DAY-AHEAD BIDDING OF ENERGY HUBS IN THE JOINT ELECTRICITY AND CARBON MARKET

In this section, a typical EH model is introduced, together with its bidding scheme in the joint electricity and carbon market.

2.1 Energy Hub Models

An EH is typically treated as a multiple-input and multiple-output energy conversion system, including the functions of conversion, storage, and consumption (Zhao et al., 2020). Considering the electrification of buildings, transportation, and industries in the coming decades, there exist electrical and thermal hubs in the system (Oskouei et al., 2021). The input of the EH is the utility grid (UG), PV generation, and natural gas. The energy conversion is realized by the combined heat and power (CHP) unit and air-conditioning. The AC/DC conversion in the electrical hub is realized by the bi-directional AC/DC converters. The battery and thermal ESSs are used to store electricity and thermal.

2.2 Day-Ahead Bidding Progress of Energy Hubs

The EHO is to manage the conversion, storage, and utilization processes in the EHs while participating in both electricity and carbon markets. The EHO acts as the price taker in both markets. The bidding procedure for the EHO is shown in **Figure 1**.

As shown in **Figure 1**, the EHO can buy and sell electricity in the day-ahead and real-time markets. The carbon permit is purchased in the day-ahead and real-time carbon markets. In the day-ahead bidding, the electricity and carbon prices are given, while the real-time electricity and carbon prices, together with PV output, demand, and ambient temperature, are uncertain, which is depicted by a scenario tree with uncertain probability density functions (PDFs).

3 DISTRIBUTIONALLY ROBUST BIDDING PROBLEM FORMULATION

The optimal day-ahead bidding problem for EHs is formulated as a bi-objective two-stage distributionally robust optimization problem in this section, including the day-ahead operation and real-time operation recourse.

3.1 Two-Stage Distributionally Robust Chance-Constrained Programming Problem

A two-stage distributionally robust chance constrained optimization problem is shown as follows:

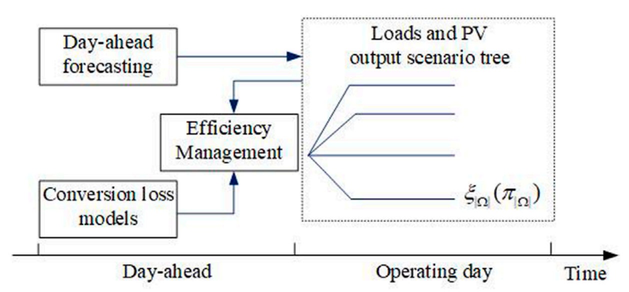

FIGURE 1 | Bidding process in the joint electricity and energy market.

$$\min_{\mathbf{x}\in\mathbf{X}} f(\mathbf{x}) + \max_{\mathbb{P}\in\mathcal{P}}\{\rho\mathbb{E}_{\omega\sim\mathbb{P}}[\mathcal{Q}(\mathbf{x},\omega)] + (1-\rho)\,\mathrm{CVaR}_{\alpha}[\mathcal{Q}(\mathbf{x},\omega)]\}, \tag{1}$$

where $\mathbf{x}$ represents the day-ahead bidding strategy of EHO, including the electricity and carbon permit purchase plan, as shown in **Eq. 6**. $\mathbf{X}$ is the first-stage constraint set, including box constraints **Eqs 7**, **8**. ρ is the weight factor between the expected value and conditional value at risk (CVaR), which is employed as a measure of the tail risk with the given confidence level α. The choice of ρ depends on the risk preference of the EHO. For instance, if the EHO is only concerned about the expected cost minimization, ignoring the potential trading risk in extreme conditions, ρ is set to be 0. The calculation of CVaR is shown as follows:

$$\mathrm{CVaR}_{\alpha}\,[\mathcal{Q}(\mathbf{x},\omega)] = \min_{\eta}\left\{\left(\eta + \frac{1}{1-\alpha}\,\mathbb{E}\,[(\mathcal{Q}\,[(\mathbf{x},\omega)-\eta]^{+}]\right\}, \tag{2}$$

where η is the value at risk (VaR). For more details on VaR refer to Rockafellar and Uryasev (2000).

$\mathbb{P}$ is the probability within the following ambiguity set:

$$\mathcal{P} := \left\{ \mathbb{P}\in\mathcal{M}(\Xi,\mathcal{F}) \left| \begin{array}{c} \mathbb{P}(\xi\in\Omega)=1 \\ \sum_{\omega\in\Omega}|\pi_{\omega}-\pi_{0,\omega}|\le\tau \\ \sum_{\omega\in\Omega}\pi_{\omega}\xi_{\omega}=\xi_0 \end{array} \right. \right\}, \tag{3}$$

where π_{ω} and $\pi_{0,\omega}$ are the real probability density and nominal probability density of scenario ω. As shown in **Eq. 3**, the ambiguity set only limits the density function on the given support set Ω. The mean value of prices and renewable energy outputs is preserved by the third line of **Eq. 3** (Liu et al., 2021). This ambiguity set is further represented by the compact format $\mathbf{G}\omega \le \mathbf{e}$. $\mathcal{Q}(\mathbf{x},\omega)$ is the following recourse problem to capture the optimal decision of EHOs in real-time operation, with the given day-ahead bidding plan and uncertainties.

$$\mathcal{Q}(\mathbf{x},\omega) := \min_{\mathbf{y}_{\omega}\in\mathbf{Y}(\mathbf{x},\omega)}\{\mathbf{q}^{T}\mathbf{y}_{\omega}|\mathbf{D}\mathbf{y}_{\omega}\ge\mathbf{h}_{\omega}-\mathbf{T}_{\omega}\mathbf{x}\}, \tag{4}$$

where $\mathbf{D}\mathbf{y}_{\omega}\ge\mathbf{h}_{\omega}-\mathbf{T}_{\omega}\mathbf{x}$ is the compact representation of **Eqs 10–12**, **14–33**.

The following distributionally robust chance constraint is introduced to balance the feasibility of the recourse problem and uncertainties:

$$\Pr_{\omega\sim\Omega}\{\mathbf{E}\mathbf{y}_{\omega}+\mathbf{F}\xi_{\omega}\le\mathbf{g}_{\omega}\}\ge 1-\beta, \tag{5}$$

where β is the confidential level of the feasibility of the constraint (**Eq. 13**). The detailed formulation on the first stage and second stage optimization problems are given in the following subsections.

3.2 Day-Ahead Bidding Optimization

The first stage optimization is to minimize the total cost in the day-ahead market, including the electricity and carbon cost, as follows:

$$f(\mathbf{x}) = \sum_{t\in\mathcal{T}}[\lambda_{\mathrm{DA}}(t)P_{\mathrm{DA}}(t) + \mu_{\mathrm{DA}}(t)\Phi_{\mathrm{DA}}(t)], \tag{6}$$

where $\lambda_{\mathrm{DA}}(t)$ and $\mu_{\mathrm{DA}}(t)$ are the electricity and carbon prices in the day-ahead markets. The day-ahead bidding plan is limited by the following constraints:

$$P_{\mathrm{UG,min}} \le P_{\mathrm{DA}}(t) \le P_{\mathrm{UG,max}}, \forall t, \tag{7}$$

$$\Phi_{\mathrm{C,min}} \le \Phi_{\mathrm{DA}}(t) \le \Phi_{\mathrm{C,max}}, \forall t, \tag{8}$$

where $P_{\mathrm{UG,\,min}}$, $P_{\mathrm{UG,\,max}}$, $\Phi_{\mathrm{C,\,min}}$, and $\Phi_{\mathrm{C,\,max}}$ are the minimal and maximal electricity and carbon purchasing limits in the day-ahead and real-time markets.

3.3 Real-Time Operation Optimization

Real-time operation optimization is to minimize the real-time operational cost by optimal scheduling of the generation, conversion, and consumption processes within EHs. The objective function in the second stage optimization is depicted as follows:

$$\begin{aligned}\mathbf{q}^T\mathbf{y}_\omega = \sum_{t\in\mathcal{T}} \{ & c_{\mathrm{GAS}}\left[v_{\mathrm{CHP},\omega}(t) + v_{\mathrm{GAS},\omega}(t)\right] + c_{\mathrm{PV}} p_{\mathrm{PV},\omega}(t) \\ & + \lambda_{\mathrm{RT},\omega} p_{\mathrm{RT},\omega}(t) + c_{\mathrm{ES,CH}} p_{\mathrm{ES,CH},\omega}(t) \\ & + c_{\mathrm{ES,DC}} p_{\mathrm{ES,DC},\omega}(t) + \mu_{\mathrm{RT},\omega}(t)\,\phi_{\mathrm{RT},\omega}(t)\},\end{aligned} \tag{9}$$

where subscription ω represents for scenario ω. $\lambda_{\mathrm{RT},\omega}(t)$ and $\mu_{\mathrm{RT},\omega}(t)$ are the real-time electricity and carbon prices in the electricity and carbon markets. $p_{\mathrm{RT}}(t)$ and $\phi_{\mathrm{RT}}(t)$ are the real-time power between the EH and UG and carbon permit purchased, respectively. $c_{\mathrm{ES,CH}}$ and $c_{\mathrm{ES,DC}}$ are the charging and discharging cost of battery energy systems (BESs), respectively. $p_{\mathrm{ES,CH},\omega}(t)$ and $p_{\mathrm{ES,DC},\omega}(t)$ are the charging and discharging rates of the BES, respectively. c_{GAS} is the price of natural gas. $v_{\mathrm{CHP},\omega}(t)$ and $v_{\mathrm{GAS},\omega}(t)$ are the gas consumption of CHP and gas boiler, respectively.

The constraints for within the EHs include the thermal, electrical, conversion, storage, and carbon emission constraints, as shown in the following subsections.

3.3.1 Constraints for the Thermal Hub

The energy balance equations in the heating and cooling hubs of the EH are depicted as follows:

$$\begin{aligned} & q_{\mathrm{HVAC,TD},\omega}(t) + q_{\mathrm{TD},\omega}(t) + q_{\mathrm{AC},\omega}(t) + q_{\mathrm{HS,CH},\omega}(t) \\ & \quad = q_{\mathrm{GAS},\omega}(t) + q_{\mathrm{CHP},\omega}(t) + q_{\mathrm{HS,DC},\omega}(t), \forall t, \omega,\end{aligned} \tag{10}$$

$$\begin{aligned} & q_{\mathrm{HVAC,CD},\omega}(t) + q_{\mathrm{CD},\omega}(t) \\ & \quad = q_{\mathrm{CS,DC},\omega}(t) + q_{\mathrm{IAC},\omega}(t) + q_{\mathrm{CE},\omega}(t), \forall t, \omega,\end{aligned} \tag{11}$$

where $q_{\mathrm{HVAC,TD},\omega}(t)$ and $q_{\mathrm{HVAC,CD},\omega}(t)$ are the heating and cooling demand to control the indoor room temperature, respectively. $q_{\mathrm{TD},\omega}(t)$ and $q_{\mathrm{CD},\omega}(t)$ are the heating and cooling demand, respectively. $q_{\mathrm{AC},\omega}(t)$ and $q_{\mathrm{CE},\omega}(t)$ are the heating consumption and cooling output of the absorption chiller, respectively. $q_{\mathrm{CHP},\omega}(t)$ and $q_{\mathrm{GAS},\omega}(t)$ are the heating output of the CHP and gas boiler, respectively. $q_{\mathrm{HS,CH},\omega}$ and $q_{\mathrm{HS,DC},\omega}(t)$ are the charging and discharging rates of heating energy storage (HES), respectively. $q_{\mathrm{CS,CH},\omega}$ and $q_{\mathrm{CS,DC},\omega}(t)$ are the charging and discharging rates of cooling energy storage (CES), respectively. $q_{\mathrm{IAC},\omega}(t)$ is the cooling output of the inverter air-conditioning system.

Eqs 10, **11** depict the energy balance on the heating hub and cooling hub, respectively.

The indoor room temperature of a cluster of buildings is managed *via* the consumption of heating and cooling from the EH, as shown in **Figure 2**. Based on Fourier's law, the relationship between the heating/cooling loads and indoor room temperature can be approximated by the following linear equations (Zhang et al., 2018):

$$\begin{aligned}\frac{q_{\mathrm{HVAC,TD},\omega}(t) - q_{\mathrm{HVAC,CD},\omega}(t)}{\Delta t} = c_{\mathrm{air}} & \frac{\Theta_{\mathrm{in},\omega}(t) - \Theta_{\mathrm{in},\omega}(t-\Delta t)}{\Delta t} \\ & - \frac{\Theta_{\mathrm{am},\omega}(t) - \Theta_{\mathrm{in},\omega}(t)}{R_{\mathrm{T}}}, \forall t, \omega,\end{aligned} \tag{12}$$

where $\Theta_{\mathrm{in},\omega}(t)$ and $\Theta_{\mathrm{am},\omega}(t)$ are the indoor temperature and ambient temperature, respectively. c_{air} is the air heating capacity (kWh/°C), and R_{T} is the thermal resistance of the building envelope (°C/kW). To guarantee the thermal service quality, the indoor room temperature should be guaranteed within the given range as follows:

$$\Theta_{\mathrm{in,min}} \le \Theta_{\mathrm{in},p,k}(t) \le \Theta_{\mathrm{in,max}}, \forall t, \omega, \tag{13}$$

where $\Theta_{\mathrm{in,min}}$ and $\Theta_{\mathrm{in,max}}$ are the minimal and maximal limitations for the indoor room temperature, respectively.

3.3.2 Constraints of the Electrical Hub

In the electrical systems, the power balance equations on the AC bus and DC bus of the electrical hub can be depicted as follows:

$$\begin{aligned} & P_{\mathrm{DA}}(t) + p_{\mathrm{RT},\omega}(t) + p_{\mathrm{CHP},\omega}(t) + \eta_{\mathrm{BIC}} p_{\mathrm{DC2AC},\omega}(t) \\ & \quad = p_{\mathrm{AC},\omega}(t) + p_{\mathrm{AC2DC},\omega}(t), \forall t, \omega,\end{aligned} \tag{14}$$

$$\begin{aligned} & p_{\mathrm{ES,DC},\omega}(t) - p_{\mathrm{ES,CH},\omega}(t) + \eta_{\mathrm{BIC}} p_{\mathrm{AC2DC},\omega}(t) + p_{\mathrm{PV},\omega}(t) \\ & \quad = p_{\mathrm{DC},\omega}(t) + p_{\mathrm{DC2AC},\omega}(t) + p_{\mathrm{IAC},\omega}(t) + p_{\mathrm{CS},\omega}, \forall t, \omega,\end{aligned} \tag{15}$$

where $p_{\mathrm{CHP},\omega}(t)$ is the electric output of CHP, $p_{\mathrm{AC2DC},\omega}(t)$ and $p_{\mathrm{DC2AC},\omega}(t)$ are the power transferred from the AC bus to DC bus and DC bus to AC bus, respectively. $p_{\mathrm{AC},\omega}(t)$ and $p_{\mathrm{DC},\omega}(t)$ are the AC load and DC load, respectively. $p_{\mathrm{IAC},\omega}(t)$ is the electricity consumption of the inverter air-conditioning system. η_{BIC} is the efficiency of the bidirectional converter (BIC). **Eqs 14**, **15** depict the power balance on the AC bus and DC bus of the electrical hub, respectively.

The limitations for power exchange between the UG and EH and power transferring on the BIC are shown as follows:

$$P_{\mathrm{UG,min}} \le p_{\mathrm{RT},\omega}(t) \le P_{\mathrm{UG,max}}, \forall t, \omega, \tag{16}$$

$$P_{\mathrm{UG,min}} \le p_{\mathrm{RT},\omega}(t) + P_{\mathrm{DA}}(t) \le P_{\mathrm{UG,max}}, \forall t, \omega, \tag{17}$$

$$0 \le P_{\mathrm{DC2AC},\omega}(t) \le I_{\mathrm{DC2AC},\omega}(t)\, P_{\mathrm{BIC,max}}, \forall t, \omega, \tag{18}$$

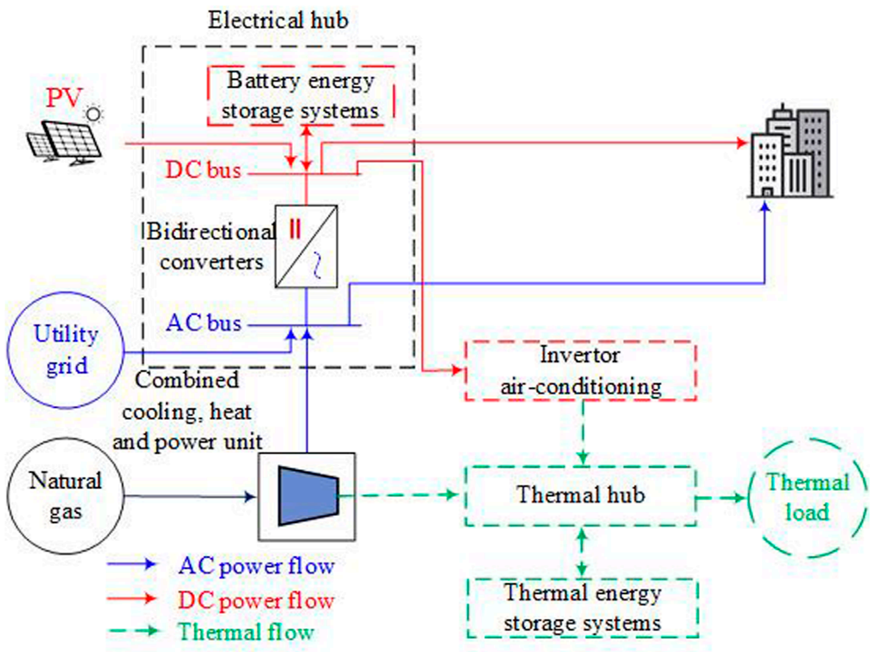

FIGURE 2 | Illustrative figure for the energy hub.

$$0 \le P_{\mathrm{AC2DC},\omega}(t) \le \left(1 - I_{\mathrm{DC2AC}\omega}(t)\right) P_{\mathrm{BIC,max}}, \forall t, \omega, \tag{19}$$

where $P_{\mathrm{BIC,max}}$ is the capacity of the BIC. $I_{\mathrm{DC2AC},\omega}(t)$ is a binary variable, indicating the operating status of BICs, i.e., 1 if BIC is on the inverter mode and 0 on the rectifier mode.

Eqs 16, **17** represent the power range limitation on the day-ahead and real-time power exchange between the EH and utility grid. **Eqs 18**, **19** are the constraints for power conversion from the DC bus to AC bus and AC bus to DC bus, respectively. I_{DC2AC} forces the unidirection of power conversion on the BIC.

3.3.3 Constraints of Energy Conversion

The energy conversion constraints are to depict the relationship among energy carriers within the EH, which can be depicted as the following linear functions (Zhao et al., 2020):

$$v_{\mathrm{CHP},\omega}(t)\eta_{\mathrm{CHPe}} = p_{\mathrm{CHP},\omega}(t), \forall t, \omega, \tag{20}$$

$$v_{\mathrm{CHP},\omega}(t)\eta_{\mathrm{CHPh}} = q_{\mathrm{CHP},\omega}(t), \forall t, \omega, \tag{21}$$

$$v_{\mathrm{GAS},\omega}(t)\eta_{\mathrm{GAS}} = q_{\mathrm{GAS},\omega}(t), \forall t, \omega, \tag{22}$$

$$p_{\mathrm{IAC},\omega}(t)\eta_{\mathrm{IAC}} = q_{\mathrm{IAC},\omega}(t), \forall t, \omega, \tag{23}$$

$$p_{\mathrm{CS},\omega}(t)\eta_{\mathrm{PCS}} = q_{\mathrm{CS,CH},\omega}(t), \forall t, \omega, \tag{24}$$

$$q_{\mathrm{AC},\omega}(t)\eta_{\mathrm{AC}} = q_{\mathrm{CE},\omega}(t), \forall t, \omega, \tag{25}$$

where η_{CHPe} and η_{CHPh} are the electricity and heat conversion efficiency of CHP, respectively. η_{GAS}, η_{IAC}, η_{AC}, and η_{PCS} are the conversion efficiencies of the gas boiler, absorption chiller, air conditioner, and ice storage air conditioner, respectively.

Eq. 20 shows the energy conversion from gas to electricity. The conversion from gas to heating is depicted by **Eqs 21**, **22**, using the CHP and gas boiler, respectively. The conversion from electricity to cooling is depicted by **Eqs 23**, **24**, using the air conditioner and ice storage air conditioner, respectively. The conversion from heating to cooling is shown in **Eq. 25**. It should be noted that these linear functions might be oversimplified, especially for the CHP. If heat recovery and other processes are considered, their equations can be replaced by more accurate convex or non-convex models, balancing the optimality and feasibility (Dai et al., 2017).

3.3.4 Constraints of Energy Storage Systems

Considering the self-discharge, charge, and discharge of processes, the constraints for the ESSs, including BES, CES, and HES, are represented as follows (Zhao et al., 2018):

$$0 \le y_{\mathrm{DC},\omega}(t) \le y_{\mathrm{DC,max}}, \forall t, \omega, \tag{26}$$

$$0 \le y_{\mathrm{CH},\omega}(t) \le y_{\mathrm{CH,max}}, \forall t, \omega, \tag{27}$$

$$y_{\mathrm{ES,min}} \le y_{\mathrm{ES},\omega}(t) \le y_{\mathrm{ES,max}}, \forall t \in \mathcal{T}, \tag{28}$$

$$y_{\mathrm{ES},\omega}(t) = \eta_y y_{\mathrm{ES},\omega}(t-\Delta t) + y_{\mathrm{CH},\omega}(t)\eta_{y,\mathrm{CH}}\Delta t - \frac{y_{\mathrm{DC},\omega}(t)\Delta t}{\eta_{y,\mathrm{DC}}}, \forall t, \omega, \tag{29}$$

$$y_{\mathrm{CH},\omega} \le I_{\mathrm{CH},\omega}(t)\, y_{\mathrm{CH,max}} \forall t,\omega, \tag{30}$$

$$y_{\mathrm{DC},\omega} \le \left(1 - I_{\mathrm{CH},\omega}(t)\right) y_{\mathrm{DC,max}} \forall t,\omega, \tag{31}$$

$$y_{\mathrm{ES},\omega}(T) = y_{\mathrm{ES}}(0), \forall \omega, \tag{32}$$

where $y_{\mathrm{DC}}(t)$, $y_{\mathrm{CH}}(t)$, and $y_{\mathrm{ES}}(t)$ represent the discharging, charging, and energy status of BES, HES, and CES, respectively. $I_{\mathrm{CH},k}(t)$ is a binary variable, indicating the charging and discharging status, respectively. $\eta_{y,\mathrm{CH}}$, $\eta_{y,\mathrm{DC}}$, and η_y represent the charging, discharging, and self-discharging efficiency of ESSs, respectively. $y_{\mathrm{DC,max}}$, $y_{\mathrm{CH,max}}$, $y_{\mathrm{ES,min}}$, and $y_{\mathrm{ES,max}}$ are the limitations for the discharging, charging, and energy status, respectively.

Eqs 26–28 are the limitations on the discharging, charging, and energy status of ESSs, respectively. The energy status dynamic is shown in **Eq. 29**. **Eqs 30–32** enforce that the ESS can only be either charging or discharging within each period. After the operation, the energy status should be the same as the initial status, as depicted by **Eq. 32**.

3.3.5 Constraints of Carbon Emission

The carbon emissions are generated by the utilized electricity and gas, which should be less than the purchased carbon permit in the day-ahead market and real-time market, as follows:

$$\begin{aligned}\sum_{t\in\mathcal{T}} \left[P_{\mathrm{DA}}(t) + p_{\mathrm{RT}}(t)\right] v_{\mathrm{ele}} + \left[v_{\mathrm{CHP},\omega}(t) + v_{\mathrm{GAS},\omega}(t)\right] v_{\mathrm{gas}} \\ \le \sum_{t\in\mathcal{T}} \left[\Phi_{\mathrm{DA}}(t) + \phi_{\mathrm{RT},\omega}(t)\right],\end{aligned} \tag{33}$$

where v_{ele} and v_{gas} are the carbon emission co-efficients of electricity and natural gas, respectively.

4 DETERMINISTIC REFORMULATION

As shown in **Eqs 1–5**, the formulated problem is a two-stage distributionally robust jointed chance-constrained programming problem. This problem cannot be solved directly as the density function is uncertain. It is further reformulated as its deterministic counterpart, which is a mixed-integer linear programming problem.

4.1 Deterministic Reformulation of Jointed Chance Constraints

To reformulate the joint chance constraints (**Eq. 5**) as a deterministic constraint, an indicator function is introduced as follows, to show whether $\mathbf{y}$ is feasible or not under scenario ω :

$$I_\omega = \begin{cases} 0, \mathbf{E}\mathbf{y}_\omega + \mathbf{F}\xi_\omega \le \mathbf{g}_\omega, \\ 1, \mathbf{E}\mathbf{y}_\omega + \mathbf{F}\xi_\omega > \mathbf{g}_\omega \end{cases} \tag{34}$$

Using the indicator function (**Eq. 34**), the joint chance constraint (**Eq. 5**) can be reformulated as the following constraints:

$$\sum_{\omega\in\Omega} I_\omega \pi_\omega \le \beta, \tag{35}$$

$$\mathbf{E}\mathbf{y}_\omega + \mathbf{F}\xi_\omega \le \mathbf{g}_\omega + I_\omega M, \tag{36}$$

where M is a scalar big enough to guarantee the feasibility of problem (**Eq. 4**), when I_ω is activated to 1. Based on the ambiguity set (3), constraint (**Eq. 35**) can be further reformulated as the following constraint:

$$\begin{aligned} &\mathbf{e}^{\mathrm{T}}\gamma \le \beta \\ &\mathbf{G}^{\mathrm{T}}\gamma \ge \mathbf{b}(I_\omega), \\ &\gamma \ge 0 \end{aligned} \tag{37}$$

where γ is the Lagrange multiplier of $\mathbf{G}\omega \le \mathbf{e}$, that is, the ambiguity set (**Eq. 3**), and $\mathbf{b}(I_\omega)$ is the vector to represent the $\sum_{\omega\in\Omega} I_\omega \pi_\omega$.

It can be seen that after the reformulation (**Eq. 37**), the jointed chance constraint can be solved by its deterministic counterpart.

4.2 Deterministic Reformulation of Second-Stage Optimization Problems

The expected CVaR value in **Eq. 1**, that is, $\max_{\mathbb{P}\in\mathcal{P}}\{\rho\mathbb{E}_{\omega\sim\mathbb{P}}[\mathcal{Q}(\mathbf{x},\omega)] + (1-\rho)\mathrm{CVaR}_\alpha[\mathcal{Q}(\mathbf{x},\omega)]\}$, can be reformulated based on Lagrange duality, as the following problem:

$$\begin{aligned} \min_{z,v,\eta,z_\omega^+,z_\omega^-,\kappa} \ & \tau z + (1-\rho)\eta + \xi_0^{\mathrm{T}}\kappa + \sum_\omega \pi_{0,\omega}\left(z_\omega^+ - z_\omega^-\right) + v \\ \text{s.t.} \ & \mathbf{q}^{\mathrm{T}}\mathbf{y}_\omega + \frac{1-\rho}{1-\beta} v_\omega \le z_\omega^+ - z_\omega^- + v + \xi_\omega^{\mathrm{T}}\kappa, \forall\omega \\ & z_\omega^+ - z_\omega^- \le z, \forall\omega \\ & \mathbf{q}^{\mathrm{T}}\mathbf{y}_\omega - \eta \le v_\omega, \forall,\omega \\ & z_\omega^+, z_\omega^-, v_\omega \ge 0, \forall\omega \end{aligned} \tag{38}$$

where $z, v, \eta, z_\omega^+, z_\omega^-, and \kappa$ are the auxiliary variables.

After the deterministic reformulation of the jointed chance constraints and the second-stage optimization problem, problems **(1)**–**(5)** can be treated as the following mixed-integer linear programming problem:

$$\begin{aligned} \min_{\mathbf{x},\mathbf{y}_\omega,I_\omega,z,v,\eta,z_\omega^+,z_\omega^-,\kappa,\gamma} \ & \tau z + (1-\rho)\eta + \xi_0^{\mathrm{T}}\kappa \\ & + \sum_\omega \pi_{0,\omega}\left(z_\omega^+ - z_\omega^-\right) + v \\ \text{s.t.} \ & \mathbf{D}\mathbf{y}_\omega \ge \mathbf{h}_\omega - \mathbf{T}_\omega\mathbf{x}, \forall\omega \\ & \mathbf{E}\mathbf{y}_\omega + \mathbf{F}\xi_\omega \le \mathbf{g}_\omega + I_\omega M, \forall\omega \\ & \mathbf{q}^{\mathrm{T}}\mathbf{y}_\omega + \frac{1-\rho}{1-\beta} v_\omega \le z_\omega^+ - z_\omega^- + v + \xi_\omega^{\mathrm{T}}\kappa, \forall\omega \\ & z_\omega^+ - z_\omega^- \le z, \forall\omega \\ & \mathbf{q}^{\mathrm{T}}\mathbf{y}_\omega - \eta \le v_\omega, \forall\omega \\ & z_\omega^+, z_\omega^-, v_\omega \ge 0, \forall\omega \\ & \mathbf{e}^{\mathrm{T}}\gamma \le \beta \\ & \mathbf{G}^{\mathrm{T}}\gamma \ge \mathbf{b}(I_\omega) \\ & \gamma \ge 0 \end{aligned} \tag{39}$$

Problem **(39)** can be solved by offshore commercial solvers, e.g., Gurobi and Cplex.

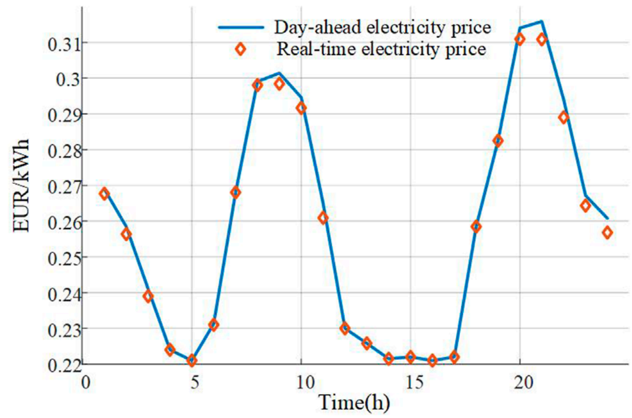

FIGURE 3 | Prices in the day-ahead and forecast prices in the real-time electricity markets.

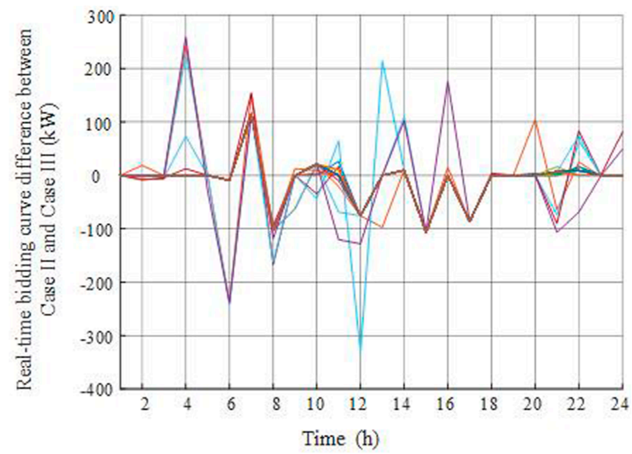

FIGURE 5 | Real-time bidding curve differences in different scenarios between case II and case III.

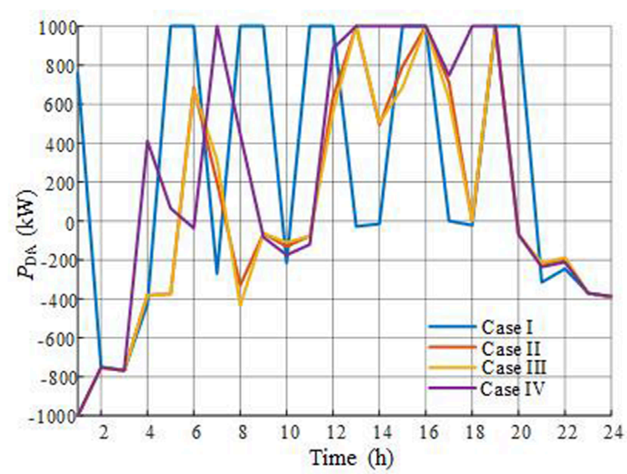

FIGURE 4 | Day-ahead bidding curves under different cases.

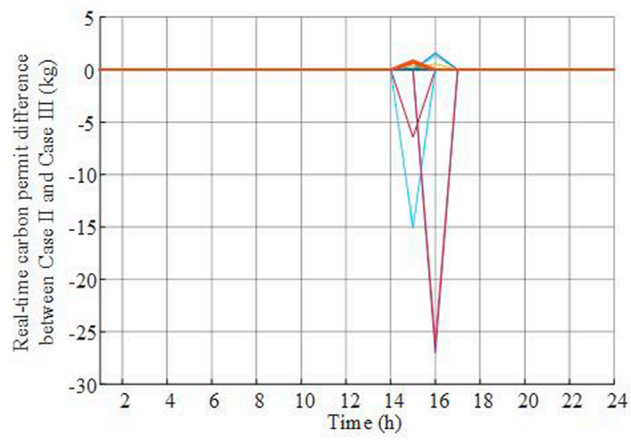

FIGURE 6 | Real-time bidding curve differences in different scenarios between case II and case III.

5 CASE STUDY

5.1 Case Description

To verify the effectiveness of the proposed bidding strategy, an EH test system is proposed, as shown in **Figure 2**. The bidirectional AC/DC converter is used to realize the AC/DC conversion in the electrical hub. The electrical load, heat load, and cooling load profiles are obtained from Sadeghian et al. (2017). The day-ahead electricity price and expected real-time electricity price profiles are obtained from energy market prices in Omie (2022), as shown in **Figure 3**, and carbon prices are extracted from EU Carbon Permits (Tradingeconomics, 2022a). For the second stage optimization, 100 scenarios are generated, including the electrical prices, loads, PV output, and ambient temperature. α is

TABLE 1 | Simulation results under different cases.

Case	I	II	III	IV	V
$f(\mathbf{x})$(\$)	5027.94	5136.68	5141.38	5128.93	5103.22
$\sum_t P_{\mathrm{DA}}(t)$(kWh)	6943.29	1385.68	1166.83	5346.13	2471.69
$\mathbb{E}_{\mathbb{P}_0}(\sum_t p_{\mathrm{RT}}(t))$(kWh)	9874.70	15421.00	15641.00	11264.33	14335.97
$\sum_t \Phi_{\mathrm{DA}}(t) + \mathbb{E}_{\mathbb{P}_0}(\sum_t \phi_{\mathrm{RT}}(t))$(kg)	5419.84	5420.35	5421.04	5365.70	5421.71

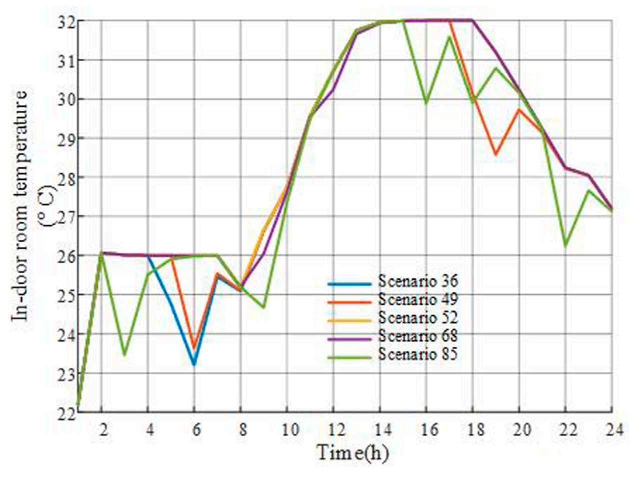

FIGURE 7 | Indoor room temperature in selected scenarios.

set to 0.95. Other parameter settings are obtained from Zhao et al. (2020).

Numerical simulations were carried out on a desktop with an Intel Xeon Gold 6226R CPU and 128 GB of RAM. The MILP problem in **Eq. 39** is solved by the commercial solver Gurobi with branch-and-cut and simplex methods.

To show the effectiveness of the proposed method, four different cases are performed as follows:

- Case I: The uncertainties have not been considered.
- Case II: $\tau = 0$, $\beta = 0$, and $\rho = 0.5$.
- Case III: $\tau = 0.1$, $\beta = 0$, and $\rho = 0.5$.
- Case IV: $\tau = 0.1$, $\beta = 0.1$, and $\rho = 0.5$.
- Case V: $\tau = 0$, $\beta = 0$, and $\rho = 1$.

5.2 Result Analysis

The simulation results under different cases are shown in **Table 1**, and the day-ahead bidding curves of the EHO in the day-ahead market are shown in **Figure 4**.

5.2.1 Impacts of Uncertainties

As shown in **Table 1**, an increase in the operational cost from 5027.94 \$ to 5136.68 \$ can be induced including uncertainties of PV output, demand, and ambient temperature. The day-ahead bidding curves of case I and case II vary, as shown in **Figure 4**, especially during the (0:00, 1:00). In case 1, the uncertainties have not been considered, which means forecast prices in the real-time market are accurate without bias, so it is specific for the EHO whether there is a need for arbitrage or not. In other words, the EHO tends to purchase as much electricity as possible, in the day-ahead market during time slots when the electricity price in the day-ahead market is lower than in the real-time market, e.g., (5:00, 6:00) and (8:00, 9:00). The purchased electricity during these time slots has reached the given upper limit, that is, 1000 kW.

To explore the effectiveness of the risk-averse, the risk factor ρ is set to be 1 in case V. In comparison with case II, the potential trading risk, which can be incurred in the extreme condition, is neglected by the EHO to search for a lower expected cost.

5.2.2 Impacts of Distributionally Robust Uncertainties

The real-time bidding and carbon permit trading difference curves between case II and case III are shown in **Figures 5**, **6**. The uncertainties of the probability distribution are considered, and the worst condition is found by the optimization process. The variance from the nominal distribution of case II increases the operational cost, which seems slight due to limited differences among scenarios. The expected electricity purchased under nominal PDF in the real-time market increased by 220 kWh in case III. An interesting observation is that even if the electricity is increased, the carbon emission almost remains the same. It indicates that the proposed bidding strategy can always reduce carbon emissions, while the electricity bidding can be adjusted accordingly.

5.2.3 Impacts of Joint Chance Constrain Relaxation

The indoor room temperature curve under scenarios 36, 49, 52, 68, and 85 are shown in **Figure 7**. In these five scenarios, the indoor room temperature has been relaxed as the highest temperature is more than 24°C, that is, the threshold temperature value. These relaxed scenarios can help reduce the carbon emission and operational cost. Furthermore, due to $\tau = 0.1$, the number of total relaxed scenarios is 5, while it should be 10 when $\tau = 0.0$, that is, the PDF is accurate.

6 CONCLUSION

In this study, a day-ahead bidding strategy is proposed for the EHO to manage its technical and economic behavior in the joint electricity and carbon market. To manage the ambiguity uncertainties of prices, loads, renewable energy output, and ambient temperature, this strategy is formulated as a two-stage distributionally robust joint chance-constrained programming problem and further been reformulated as a mixed-integer linear programming problem.

Simulations are performed on a test EH system, where the indoor room temperature can be relaxed in some scenarios. Results indicate that the proposed strategy can manage the uncertainties in the joint electricity and carbon market and reduce the operational cost and carbon emission by exploring the flexibility of the thermal demand.

DATA AVAILABILITY STATEMENT

The original contributions presented in the study are included in the article/Supplementary Material, further inquiries can be directed to the corresponding author.

AUTHOR CONTRIBUTIONS

JL completed the technical writing, idea consultation, and supervision of this work, and other authors listed also made a direct contribution to the work.

FUNDING

The work was supported in part by the consulting research project of the Chinese Academy of Engineering (2021NXZD2) and in part by the National Natural Science Foundation of China (52061635102).

REFERENCES

Brahman, F., Honarmand, M., and Jadid, S. (2015). Optimal Electrical and thermal Energy Management of a Residential Energy Hub, Integrating Demand Response and Energy Storage System. *Energy and Buildings* 90, 65–75. doi:10.1016/j.enbuild.2014.12.039

Cheng, Y., Zhang, N., Wang, Y., Yang, J., Kang, C., and Xia, Q. (2018). Modeling Carbon Emission Flow in Multiple Energy Systems. *IEEE Trans. Smart Grid* 10, 3562–3574.

Cheng, Y., Zhang, N., Zhang, B., Kang, C., Xi, W., and Feng, M. (2020). Low-carbon Operation of Multiple Energy Systems Based on Energy-Carbon Integrated Prices. *IEEE Trans. Smart Grid* 11, 1307–1318. doi:10.1109/tsg.2019.2935736

Dai, Y., Chen, L., Min, Y., Chen, Q., Hu, K., Hao, J., et al. (2017). Dispatch Model of Combined Heat and Power Plant Considering Heat Transfer Process. *IEEE Trans. Sustain. Energ.* 8, 1225–1236. doi:10.1109/tste.2017.2671744

Davatgaran, V., Saniei, M., and Mortazavi, S. S. (2018). Optimal Bidding Strategy for an Energy Hub in Energy Market. *Energy* 148, 482–493. doi:10.1016/j.energy.2018.01.174

Ding, T., Lu, R., Xu, Y., Yang, Q., Zhou, Y., Zhang, Y., et al. (2020). Joint Electricity and Carbon Market for Northeast Asia Energy Interconnection. *Glob. Energ. Interconnection* 3, 99–110. doi:10.1016/j.gloei.2020.05.002

Jadidbonab, M., Mohammadi-Ivatloo, B., Marzband, M., and Siano, P. (2020). Short-term Self-Scheduling of Virtual Energy Hub Plant within thermal Energy Market. *IEEE Trans. Ind. Electron.* 68, 3124–3136.

Li, R., Wei, W., Mei, S., Hu, Q., and Wu, Q. (2018). Participation of an Energy Hub in Electricity and Heat Distribution Markets: An Mpec Approach. *IEEE Trans. Smart Grid* 10, 3641–3653.

Liu, S., Zhao, T., and Wang, P. (2021). "Strategic Bidding for Energy Hubs Based on Hybrid Stochastic/distributionally Robust Optimization," in 2021 IEEE Power & Energy Society General Meeting (PESGM) (IEEE), 1–5. doi:10.1109/pesgm46819.2021.9637912

Lu, X., Liu, Z., Ma, L., Wang, L., Zhou, K., and Feng, N. (2020). A Robust Optimization Approach for Optimal Load Dispatch of Community Energy Hub. *Appl. Energ.* 259, 114195. doi:10.1016/j.apenergy.2019.114195

Mohammadi, M., Noorollahi, Y., Mohammadi-Ivatloo, B., and Yousefi, H. (2017). Energy Hub: From a Model to a Concept - A Review. *Renew. Sustainable Energ. Rev.* 80, 1512–1527. doi:10.1016/j.rser.2017.07.030

Olsen, D. J., Zhang, N., Kang, C., Ortega-Vazquez, M. A., and Kirschen, D. S. (2018). Planning Low-Carbon Campus Energy Hubs. *IEEE Trans. Power Syst.* 34, 1895–1907.

Omie, (2022). Day-ahead Electricity price. Available at: https://www.omie.es/en/market-results/daily/daily-market/daily-hourly-price?scope=daily&date=2022-03-01.

Oskouei, M. Z., Mohammadi-Ivatloo, B., Abapour, M., Shafiee, M., and Anvari-Moghaddam, A. (2021). Strategic Operation of a Virtual Energy Hub with the Provision of Advanced Ancillary Services in Industrial parks. *IEEE Trans. Sustain. Energ.* 12, 2062–2073. doi:10.1109/tste.2021.3079256

Rockafellar, R. T., and Uryasev, S. (2000). Optimization of Conditional Value-At-Risk. *Jor* 2, 21–41. doi:10.21314/jor.2000.038

Sadeghian, H., Athari, M. H., and Wang, Z. (2017). "Optimized Solar Photovoltaic Generation in a Real Local Distribution Network," in Power & Energy Society Innovative Smart Grid Technologies Conference (ISGT), 2017 IEEE (IEEE), 1–5. doi:10.1109/isgt.2017.8086067

Sun, W., and Huang, C. (2020). A Carbon price Prediction Model Based on Secondary Decomposition Algorithm and Optimized Back Propagation Neural Network. *J. Clean. Prod.* 243, 118671. doi:10.1016/j.jclepro.2019.118671

Tradingeconomics (2022). Carbonprice. Available at: https://tradingeconomics.com/commodity/carbon.

Yang, D., He, S., Chen, Q., Li, D., and Pandžić, H. (2019). Bidding Strategy of a Virtual Power Plant Considering Carbon-Electricity Trading. *CSEE J. Power Energ. Syst.* 5, 306–314.

Zhang, C., Xu, Y., Li, Z., and Dong, Z. Y. (2018). Robustly Coordinated Operation of a Multi-Energy Microgrid with Flexible Electric and thermal Loads. *IEEE Trans. Smart Grid* 10, 2765–2775.

Zhao, P., Gu, C., Huo, D., Shen, Y., and Hernando-Gil, I. (2019). Two-stage Distributionally Robust Optimization for Energy Hub Systems. *IEEE Trans. Ind. Inform.* 16, 3460–3469.

Zhao, T., Pan, X., Yao, S., Ju, C., and Li, L. (2020). Strategic Bidding of Hybrid Ac/dc Microgrid Embedded Energy Hubs: A Two-Stage Chance Constrained Stochastic Programming Approach. *IEEE Trans. Sustain. Energ.* 11, 116–125. doi:10.1109/tste.2018.2884997

Zhao, T., Xiao, J., Koh, L. H., Wang, P., and Ding, Z. (2018). "Strategic Day-Ahead Bidding for Energy Hubs with Electric Vehicles," in 2018 2nd IEEE Conference on Energy Internet and Energy System Integration (EI2) (IEEE), 1–6. doi:10.1109/ei2.2018.8581935

Conflict of Interest: The authors declare that the research was conducted in the absence of any commercial or financial relationships that could be construed as a potential conflict of interest.